Nonvortical Rashba Spin Structure on a Surface with C_{1h} Symmetry

Emilia Annese,[1,2,*] Takuya Kuzumaki,[1] Beate Müller,[1] Yuta Yamamoto,[1] Hiroto Nakano,[3] Haruki Kato,[3] Atsushi Araki,[3] Minoru Ohtaka,[1] Takashi Aoki,[1] Hirotaka Ishikawa,[1] Takashi Hayashida,[1] Jacek R. Osiecki,[4] Koji Miyamoto,[5] Yasuo Takeichi,[6] Ayumi Harasawa,[6] Koichiro Yaji,[6] Tetsuroh Shirasawa,[6] Koh-ichi Nittoh,[7] Wooil Yang,[8,9] Kazushi Miki,[7] Tatsuki Oda,[3] Han Woong Yeom,[8,9] and Kazuyuki Sakamoto[1,10,†]

[1]*Department of Nanomaterials Science, Chiba University, Chiba 263-8522, Japan*
[2]*Elettra Synchrotron S.C.p.A Trieste, SS 14, km 163.5, I-34149 Trieste, Italy*
[3]*Institute of Science and Engineering, Kanazawa University, Kanazawa 920-1192, Japan*
[4]*MAX-lab, Lund University, Box 118, S-22100 Lund, Sweden*
[5]*Hiroshima Synchrotron Radiation Centre, Hiroshima University, Higashi-Hiroshima 739-0046, Japan*
[6]*Institute for Solid State Physics, The University of Tokyo, Chiba 277-8581, Japan*
[7]*National Institute for Materials Science, Ibaraki 305-0044, Japan*
[8]*Center for Artificial Low Dimensional Electronic Systems, Institute for Basic Science (IBS), Pohang 790-784, Korea*
[9]*Department of Physics, Pohang University of Science and Technology (POSTECH), Pohang 790-784, Korea*
[10]*Molecular Chirality Research Center, Chiba University, Chiba 263-8522, Japan*

(Received 12 March 2016; revised manuscript received 10 May 2016; published 30 June 2016)

A totally anisotropic peculiar Rashba-Bychkov (RB) splitting of electronic bands was found on the Tl/Si(110)-(1×1) surface with C_{1h} symmetry by angle- and spin-resolved photoelectron spectroscopy and first-principles theoretical calculation. The constant energy contour of the upper branch of the RB split band has a warped elliptical shape centered at a k point located between $\bar{\Gamma}$ and the edge of the surface Brillouin zone, i.e., at a point without time-reversal symmetry. The spin-polarization vector of this state is in-plane and points almost the same direction along the whole elliptic contour. This novel nonvortical RB spin structure is confirmed as a general phenomenon originating from the C_{1h} symmetry of the surface.

DOI: 10.1103/PhysRevLett.117.016803

The determination and control of the spin structure of low-dimensional systems with high precision in both the energy and momentum space represent important goals of current solid state physics, and may imply a great possibility in technological innovations [1,2]. The spin-polarization of two-dimensional (2D) electron gas arises due to spin-orbit coupling concomitant with the breaking of spatial symmetry along the surface normal direction, and was observed on metal surfaces [3–12], transition-metal oxide surfaces [13], at interfaces between heavy element monolayer films and solid surfaces [14–19], and in a noncentrosymmetric bulk system [20]. For ideal 2D electron gases, the electronic band splits with the spin orientation locked in-plane and perpendicular to the electron momentum ($\mathbf{k}$) in a vortical structure around the center of the surface Brillouin zone (SBZ) and other time-reversal invariant momenta (TRIMs) [21] as described within the simple Rashba-Bychkov (RB) model [22]. [TRIM is a k point with time-reversal symmetry (TRS)].

The variety of electron bands and spin structures finds a comprehensive description in the generalized RB Hamiltonian within the $\mathbf{k} \cdot \mathbf{p}$ approximation, where the correlation between the symmetry of a k point and the structure is made (the symmetry of a k point results from the surface group symmetry) [23,24]. For example, a surface belonging to the plane group $p31m$ manifests the RB effect at k points of C_{3v} symmetry [17,25]. The focus in this work is on k points with C_{1h} symmetry, a symmetry with one mirror plane and without any rotational axis, which holds the potential to yield a novel spin structure [23]. In particular, the occurrence of C_{1h} symmetry at the $\bar{\Gamma}$ point, which is not realized yet, is expected to give rise to peculiar spin structure that is insensitive to backscattering and therefore along with long spin coherence [26,27]. To obtain a system whose $\bar{\Gamma}$ point has a C_{1h} symmetry and shows a RB splitting, both a substrate with a proper symmetry and an appropriate adsorbate are indispensable.

In this Letter, we report a novel spin structure of a Si(110)-(1×1) surface adsorbed with the heavy element Tl. As shown in Fig. 1(c), the presence of a mirror plane, a glide plane, and a rotation center leads the Si(110)-(1×1) ideal surface to belongs to the plane group $p2mg$, which has possibility to form a system holding a $\bar{\Gamma}$ point with C_{1h} symmetry in the k space. Tl is one of the three heaviest nonradioactive elements, and the adsorption of a heavy element with strong spin-orbit coupling induces a large RB spin splitting. Note that the two other elements Pb and Bi do not show well-ordered (1×1) periodic structure on Si(110) [28–31]. Of the observed Tl induced surfaces states, the uppermost one shows completely anisotropic dispersion with a large RB spin split along a particular direction only, and presents a constant energy contour with warped elliptical shapes centered at a nonsymmetrical k

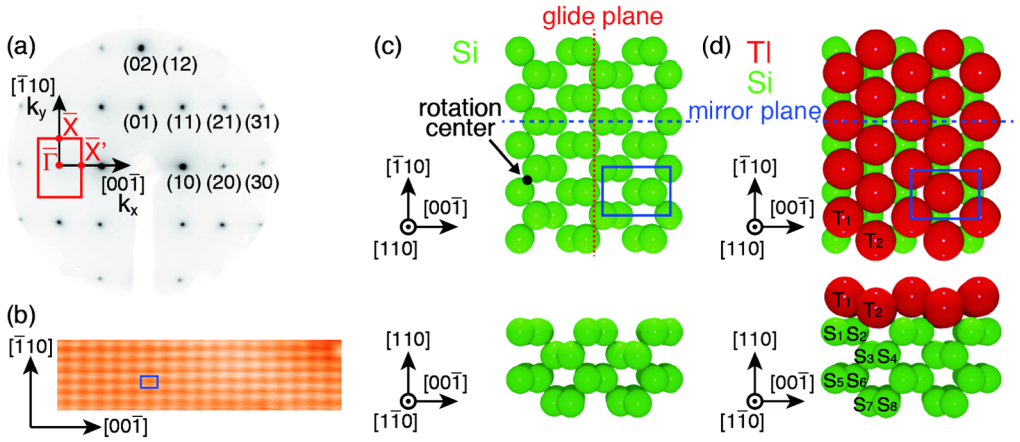

FIG. 1. (a) LEED pattern of Tl/Si(110)-(1×1); the solid rectangle indicates the SBZ, and $\bar{\Gamma}$, $\bar{X}$, and $\bar{X}'$ are the symmetry points of the SBZ. (b) A 10×2.5 nm^2 STM image of Tl/Si(110)-(1×1) obtained at a sample bias of -500 mV. The rectangle corresponds to the size of Si(110)-(1×1). Top- and side-view atomic structures of (c) the ideal Si(110)-(11) surface and (d) the Tl/Si(110)-(11) surface. The large and small circles indicate Tl and Si atoms, and the rectangles in the top view models show the (1×1) unit cell. The horizontal and vertical dashed lines in (c) and (d) indicate the mirror plane and the glide plane, respectively. The black circle in (c) shows the rotation center.

point. The spin polarization vector (**P**) of this state is in-plane, and points nearly one direction in one contour indicating the formation of a nonvortical spin structure. This novel spin structure that results from the C_{1h} symmetry of this surface is established both experimentally by photoelectron spectroscopy (PES) and theoretically by first-principles electronic structure calculations.

Angle-resolved PES (ARPES) measurements have been performed at beam line I4 of MAX-lab, Lund, Sweden, using a photon energy of 40 eV with energy and momentum resolutions of below 20 meV and below 1% of the SBZ, respectively. Spin- and angle-resolved PES (SARPES) measurements have been done at BL-19A of KEK-PF using a photon energy of 21.2 eV and a hemispherical electron analyzer equipped with a high-yield spin polarimeter based on spin-dependent very low energy electron diffraction (VLEED) [32]. One monolayer (ML) of Tl was deposited on a Si(110)-(16×2) clean surface at 450 K, prepared by annealing at 1520 K, from a Knudsen cell. All the measurements were done at 100 K.

Density functional theory (DFT) calculations were carried out by using the generalized gradient approximation (GGA) [33] in the Kohn-Sham theory [34]. The energy cutoffs of 25 and 300 Ry were used for wave functions and charge densities [35], and a repeated slab model was used for the surface calculation. The slab contains a Tl ML, 16 Si ML, and 1 H ML. The atomic positions, except those of the H atoms and the Si atoms bonded to H, were fully relaxed to an assumed criterion of atomic forces (less than 0.01 eV/Å). Each slab was separated by a vacuum space of 11.7 Å.

The atomic structure is an indispensable piece of information for discussing the electronic structure of the sample. To obtain the atomic structure of the Tl/Si(110)-(1×1) surface, we have performed low-energy electron diffraction (LEED) and scanning tunneling microscopy (STM) measurements. Figure 1(a) shows the LEED pattern obtained at a primary electron energy of 118 eV together with the SBZ, and Fig. 1(b) displays a 10×2.5 nm^2 STM image of Tl/Si(110)-(1×1). A difference in intensity at different LEED spots is clearly observed in Fig. 1(a), and one bright protrusion per unit cell is observed in Fig. 1(b). In order to acquire more detailed information about the atomic structure, we have performed LEED intensity vs voltage (I-V) measurements, and full dynamical calculations using a Barbieri–Van Hove symmetrized automated tensor LEED package [36]. (The experimentally obtained and calculated LEED I-V curves are shown in Fig. SM1 of Ref. [37].) The Pendry R factor (R_P) [38] was used to direct the automated search algorithm, and the best agreement of experimental and calculated I-V curves involved minimizing R_P.

The experimentally obtained structural model in Fig. 1(d) shows the best fit with an R_P value of 0.17, and is consistent with the optimized structural model obtained by DFT calculation as shown in Table I, where the relative positions of the two Tl atoms labeled T_1 and T_2 and the eight Si atoms labeled $S_1 - S_8$ in Fig. 1(d) are summarized. The Tl atoms organize on the Si(110) surface in two sites with different height from the outermost Si atom in accord with the observation of one bright protrusion per unit cell in STM. Further, the atomic positions of Tl atoms lead the surface structure to break the $p2mg$ symmetry of an ideal Si(110)-(1×1) surface, and to have a plane group $p1m1$ symmetry, which corresponds to a C_{1h} symmetry at the $\bar{\Gamma}$ point in k space. The loss of glide symmetry is in agreement with the observation of all LEED spots along the $[1\bar{1}0]$ direction.

Figures 2(a) and 2(b) shows results of spin-integrated ARPES measurement along the $\bar{X}'$-$\bar{\Gamma}$-$\bar{X}'$ and $\bar{X}$-$\bar{\Gamma}$ directions. Five Tl-induced states denoted as $S1$, $S1'$, $S2$, $S3$, and $S4$, which are absent on the clean Si(110) surface [39], are

TABLE I. The atom positions of Tl/Si(110)-(1 × 1) related to S_1 of Fig. 1. x, y, and z correspond to the [00$\bar{1}$], [$\bar{1}$10], and [110] directions, and LEED and DFT indicate the experimental and theoretical results. All values are given in Å.

Atom	x_{LEED}	y_{LEED}	z_{LEED}	x_{DFT}	y_{DFT}	z_{DFT}
T_1	0.68	1.92	2.82	0.57	1.92	2.80
T_2	3.23	0	1.87	3.09	0	1.88
S_1	0	0	0	0	0	0
S_2	1.41	1.92	0.02	1.34	1.92	0.00
S_3	2.74	1.92	−1.93	2.67	1.92	−1.95
S_4	4.08	0	−1.92	3.97	1.92	−1.95
S_5	0.01	0	−3.87	−0.07	0	−3.84
S_6	1.38	1.92	−3.85	1.34	1.92	−3.84
S_7	2.73	1.92	−5.79	2.68	1.92	−5.74
S_8	4.13	0	−5.78	4.01	0	−5.76

clearly observed in the bulk band gap (the edges of the bulk band projection taken from Ref. [40] are indicated by dotted lines in the figures). The lines superimposed on the band dispersion in Fig. 2(a) are the two uppermost Tl-induced occupied bands obtained theoretically along the $\bar{\Gamma}$-$\bar{X}'$ direction. The calculation indicates that $S1$ and $S1'$ originates from a unique surface state band that is split due to the RB effect, and that both bands are mainly composed of the orbitals of the lower Tl atom [T_2 in Fig. 1(d)]. Both $S1$ and $S1'$ are symmetric with respect to $\bar{\Gamma}$ and show a wave vector ($\mathbf{k}$) dependent binding energy (E_B) separation with a maximum value of $\Delta E_B = 150$ meV at $k_x = -0.28$ Å^{-1} along $\bar{X}'$-$\bar{\Gamma}$-$\bar{X}'$. Since no obvious RB split was observed experimentally for the $S2$–$S4$ bands, below we concentrate on the electronic and spin structure of $S1$ and $S1'$.

As can be seen from Figs. 2(a) and 2(b), the dispersion of $S1$ and $S1'$ is totally anisotropic; i.e., these surface states disperse first upward and then downward from $\bar{\Gamma}$ to $\bar{X}'$ while they continuously disperse downward along $\bar{\Gamma}$-$\bar{X}$ (Fig. SM2 of Ref. [37]). In order to obtain further information about the electronic structure of these anisotropic states, we have measured the constant energy contours of the uppermost state $S1$ at $E_B = 50$, 100, and 200 meV [the dotted lines in Fig. 2(c)]. The characteristic constant energy contours of the $S1$ state are the peanut shape at $E_B = 50$ meV, and warped elliptical shapes centered at $(k_x, k_y) = (\sim \pm 0.27$ Å$^{-1}, 0)$ at $E_B = 100$ and 200 meV as illustrated in Figs. 2(d)–2(f). These shapes are totally different from the constant energy contours of an ideal RB effect that show two concentric circles with their center at a TRIM such as the $\bar{\Gamma}$ point. The absence of a closed constant energy contour around $\bar{\Gamma}$ arises from the lack of rotational symmetry at this point, i.e., from the C_{1h} symmetry.

The **P** of the RB bands were revealed by DFT calculation, and verified by SARPES measurements. Figure 3(a) shows the constant energy contour at a binding energy of 0.1 eV with superimposed theoretically obtained spin orientation. Unlike the ordinary RB effect, two ellipses of opposite **P**, which are symmetric with respect to the $\bar{\Gamma}$ point, are found in the present system. **P** points toward the $-y$ direction at $k_x < 0$ and toward the $+y$ direction at $k_x > 0$ within an angle deviation of less than 16° to the x ($-x$) direction, and less than 5° to the surface normal direction (z, $-z$). This means that each elliptical constant energy contour has **P** along nearly one direction, and thus the spin structure to be nonvortical. Taking the TRS of the $\bar{\Gamma}$ point into account, the exchange of **P** at $\pm k_x$ indicates the RB split to be like an ordinary one along the $\bar{\Gamma}$-$\bar{X}'$ direction. On the other hand, the presence of nonvortical spin structures is what is not expected in the ordinary RB effect.

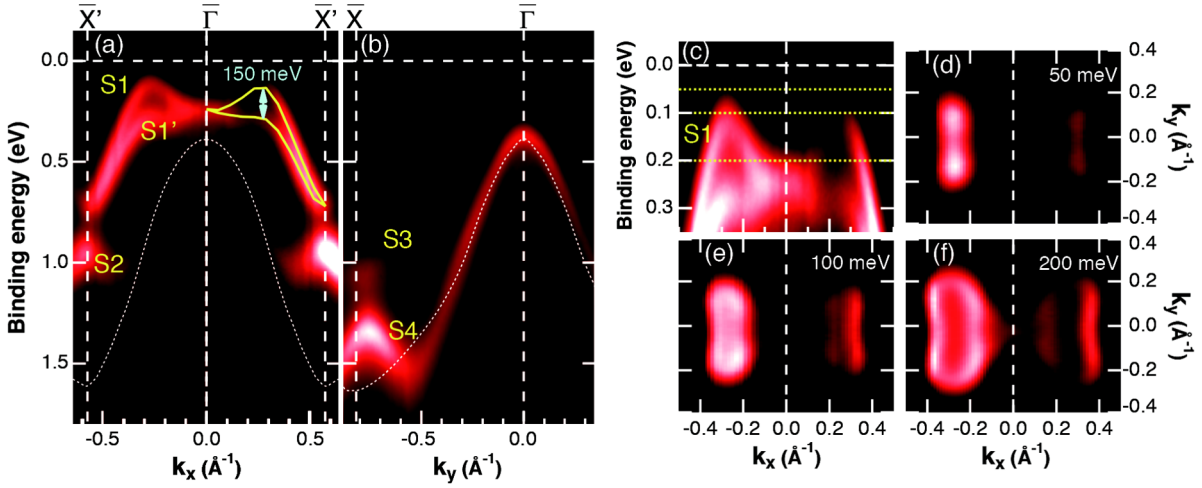

FIG. 2. Spin-integrated photoemission band from Tl/Si(110)-(1 × 1) measured at $h\nu = 40$ eV. (a) and (b) are band structures along the $\bar{X}'$-$\bar{\Gamma}$-$\bar{X}'$ and $\bar{\Gamma}$-$\bar{X}$ directions, respectively. The two upper Tl induced bands on Si(110)surface obtained theoretically along $\bar{\Gamma}$-$\bar{X}'$ are superimposed in (a). The edges of the bulk valence band projection are indicated by dotted lines in (a) and (b). (c) Spin-integrated band structure along $\bar{\Gamma}$-$\bar{X}'$, enlargement of (a). (d)–(f) are characteristic energy contours, i.e., k_x-k_y band mapping, at $E_B = 50$, 100, and 200 meV, whose energies correspond to the dotted lined in (c).

SARPES spectra measured along k_y at $k_x = 0.27$ Å^{-1} and along k_x at $k_y = 0$, at the selected points marked with filled circles in Fig. 3(b), are shown in Figs. 3(c) and 3(d). Here, the spectra were obtained with an experimental setup that is sensitive to spins with **P** parallel to the $[\bar{1}10]$ direction of Tl/Si(110)-(1×1), i.e., the y direction in Fig. 3. Thus Figs. 3(c) and 3(d) experimentally reveal that the two upper bands are spin polarized and that **P** principally points toward the $-y$ $(+y)$ direction at $k_x < 0$ $(k_x > 0)$. The spin polarization for the y component (p_y), extracted from the SARPES spectrum at $(k_x, k_y) = (-0.27\,\text{Å}^{-1}, 0)$ using $p_y = [(I_{\text{up}} - I_{\text{down}})/(I_{\text{up}} + I_{\text{down}})]/S_{\text{eff}}$,

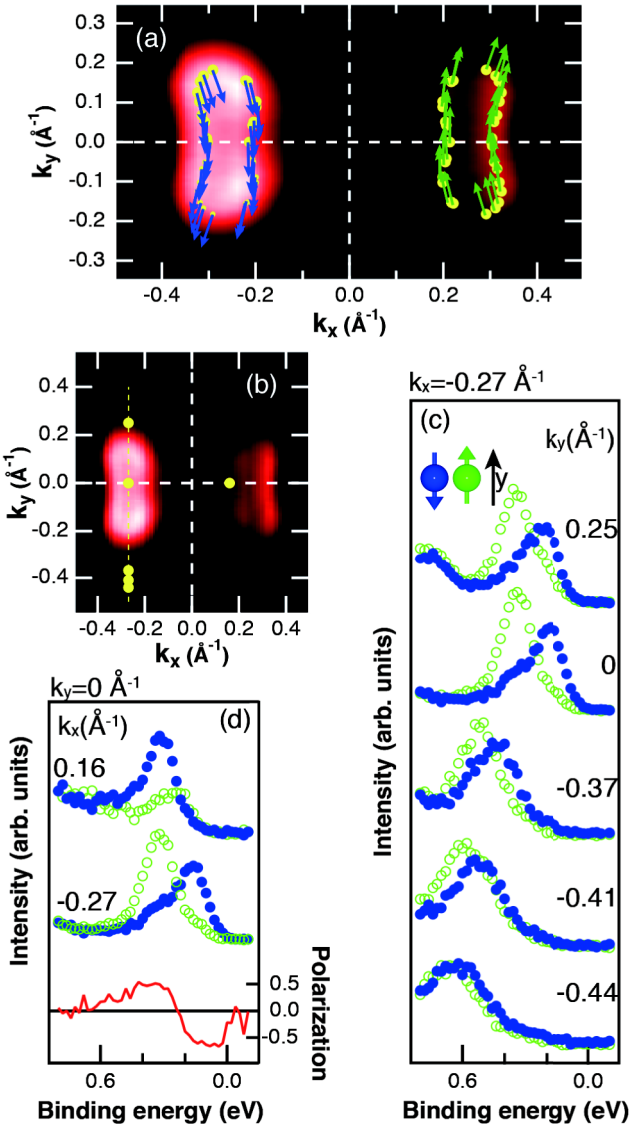

FIG. 3. (a) Constant energy contour at $E_B = 0.1$ eV superimposed with the spin structure obtained theoretically. The arrows in (a) indicate the spin orientation. (b) Filled circles showing the k points measured using SARPES. (c) and (d) are the SARPES spectra along k_y at $k_x = -0.27$ Å^{-1} and those along k_x at $k_y = 0$. The lowest spectrum in (d) shows the extracted spin polarization at $(k_x, k_y) = (-0.27$ Å$^{-1}, 0)$.

was more than 65% [Fig. 3(d)]. (I_{up} and I_{down} are the intensity of the photoelectron with opposite **P**, and $S_{\text{eff}} = 0.35$ is the effective Sherman function).

Taking into account that the $\bar{\Gamma}$-$\bar{X}'$ direction is on the mirror plane, not only the two TRIMs but all k points on this line have C_{1h} symmetry. In the case of k points with C_{1h} symmetry, the spin components parallel to the mirror plane become zero and only the component normal to the mirror plane survives [23]. This indicates that **P** is $P_y \neq 0$ and $P_x = P_z = 0$ between $\bar{\Gamma}$ and $\bar{X}'$ in the present case, and that the sign of P_y at the two $k_y = 0$ points of each constant energy contour is the same because a TRIM is necessary to reverse the **P** of a RB band to the opposite direction. Since the presence of these two k points having the same **P** direction prevents the formation of a vortical spin structure, and because the peculiar constant energy contour with its center at a non-TRIM results from the lack of rotational symmetry, we conclude that the novel RB nonvortical spin structure is a consequence of the C_{1h} symmetry of this surface. Further, this symmetry argument and the experimental results shown in Figs. 3(c) and 3(d) confirm that **P** points along one direction in each elliptical constant energy contour.

So far, the **P** of RB spins was discussed based on the contribution from only one TRIM, mainly the $\bar{\Gamma}$ point. However, the effect from more than two TRIMs ought to contribute to the **P**, and the **P** would be described by the vectorial superposition of **P** imposed from these TRIMs. In the present case, both the $\bar{\Gamma}$ and $\bar{X}'$ points should contribute to the **P**. Taking the **P** at $k_y = 0$ into account and by considering that **P** is perpendicular to **k** within a simple RB model, the effects from $\bar{\Gamma}$ and $\bar{X}'$ give $(-P_x, -P_y)$ and $(+P_x, -P_y)$ contributions, respectively, to **P** at $(k_x\langle 0, k_y\rangle 0)$. Thus the spin structure shown in Fig. 3(a) indicates that the contribution from $\bar{X}'$ is larger than that from $\bar{\Gamma}$. This means that the RB effect from $\bar{X}'$ is stronger than $\bar{\Gamma}$ on Tl/Si(110)-(1×1). This simple picture can be applied to understand the magnitude of RB effects from different TRIMs in other systems [41] as well (Fig. SM5 of Ref. [37]).

To summarize, we achieved the formation of a surface with C_{1h} symmetry that may favor the occurrence of distinct $E(k)$ spin split with a topology that is qualitatively different from the classical RB picture, by the adsorption of 1 ML of Tl on a Si(110) surface. The two upper surface states observed in ARPES, which show completely anisotropic dispersion, originate from a unique surface state band that spin split due to the RB effect along a particular direction only, and the constant energy contour of the uppermost one shows warped elliptical shapes centered at $(k_x, k_y) = (\sim \pm 0.27$ Å$^{-1}, 0)$. **P** is in-plane and points almost the same direction along the whole elliptic contour, such as $-y$ $(+y)$ for the ellipse at $k_x < 0$ $(k_x > 0)$. This characteristic nonvortical spin structure is concluded to result from the C_{1h} symmetry of the surface. The topology of the spin structure affects the spin transport efficiency [26,27], and the peculiar opposite spin band structure

observed on Tl/Si(110)-(1×1) would lead to the presence of long spin coherence along the [001] direction due to the suppression of scattering between states with opposite spin orientation.

This work was supported by the JSPS Grant-in-Aid for Scientific Research (B) 25287070 and on Innovative Areas 3D Active-Site Science 15H01041. Part of this work has been performed under the approval of the Photon Factory Program Advisory Committee (Proposal No. 2010G110). E. A. was financially supported by the FY2012 JSPS L12710. W. Y. and H. W. Y. were supported by Grant No. IBS-R014-D1.

*emiliaannese@gmail.com
†kazuyuki_sakamoto@faculty.chiba-u.jp

[1] J. Nitta, T. Akazaki, H. Takayanagi, and T. Enoki, Phys. Rev. Lett. **78**, 1335 (1997).
[2] S. Datta and B. Das, Appl. Phys. Lett. **56**, 665 (1990).
[3] Y. M. Koroteev, G. Bihlmayer, J. E. Gayone, E. V. Chulkov, S. Blügel, P. M. Echenique, and Ph. Hofmann, Phys. Rev. Lett. **93**, 046403 (2004).
[4] K. Sugawara, T. Sato, S. Souma, T. Takahashi, M. Arai, and T. Sasaki, Phys. Rev. Lett. **96**, 046411 (2006).
[5] T. Hirahara, T. Nagao, I. Matsuda, G. Bihlmayer, E. V. Chulkov, Y. M. Koroteev, P. M. Echenique, M. Saito, and S. Hasegawa, Phys. Rev. Lett. **97**, 146803 (2006).
[6] A. Takayama, T. Sato, S. Souma, and T. Takahashi, Phys. Rev. Lett. **106**, 166401 (2011).
[7] S. LaShell, B. A. McDougall, and E. Jensen, Phys. Rev. Lett. **77**, 3419 (1996).
[8] G. Nicolay, F. Reinert, S. Hüfner, and P. Blaha, Phys. Rev. B **65**, 033407 (2001).
[9] M. Hoesch, M. Muntwiler, V. N. Petrov, M. Hengsberger, L. Patthey, M. Shi, M. Falub, T. Greber, and J. Osterwalder, Phys. Rev. B **69**, 241401 (2004).
[10] D. Popović, F. Reinert, S. Hüfner, V. G. Grigoryan, M. Springborg, H. Cercellier, Y. Fagot-Revurat, B. Kierren, and D. Malterre, Phys. Rev. B **72**, 045419 (2005).
[11] H. Cercellier, C. Didiot, Y. Fagot-Revurat, B. Kierren, L. Moreau, D. Malterre, and F. Reinert, Phys. Rev. B **73**, 195413 (2006).
[12] D. Malterre, B. Kierren, Y. Fagot-Revurat, S. Pons, A. Tejeda, C. Didiot, H. Cercellier, and A. Bendounan, New J. Phys. **9**, 391 (2007).
[13] A. F. Santander-Syro, F. Fortuna, C. Bareille, T. C. Rödel, G. Landolt, N. C. Plumb, J. H. Dil, and M. Radović, Nat. Mater. **13**, 1085 (2014).
[14] C. R. Ast, J. Henk, A. Ernst, L. Moreschini, M. C. Falub, D. Pacilé, P. Bruno, K. Kern, and M. Grioni, Phys. Rev. Lett. **98**, 186807 (2007).
[15] F. Meier, H. Dil, J. Lobo-Checa, L. Patthey, and J. Osterwalder, Phys. Rev. B **77**, 165431 (2008).
[16] K. Sakamoto, T. Oda, A. Kimura, K. Miyamoto, M. Tsujikawa, A. Imai, N. Ueno, H. Namatame, M. Taniguchi, P. E. J. Eriksson, and R. I. G. Uhrberg, Phys. Rev. Lett. **102**, 096805 (2009).
[17] K. Sakamoto, H. Kakuta, K. Sugawara, K. Miyamoto, A. Kimura, T. Kuzumaki, N. Ueno, E. Annese, J. Fujii, A. Kodama, T. Shishidou, H. Namatame, M. Taniguchi, T. Sato, T. Takahashi, and T. Oguchi, Phys. Rev. Lett. **103**, 156801 (2009).
[18] K. Yaji, Y. Ohtsubo, S. Hatta, H. Okuyama, K. Miyamoto, T. Okuda, A. Kimura, H. Namatame, M. Taniguchi, and T. Aruga, Nat. Commun. **1**, 17 (2010).
[19] S. D. Stolwijk, A. B. Schmidt, M. Donath, K. Sakamoto, and P. Krüger, Phys. Rev. Lett. **111**, 176402 (2013).
[20] K. Ishizaka, M. S. Bahramy, H. Murakawa, M. Sakano, T. Shimojima, T. Sonobe, K. Koizumi, S. Shin, H. Miyahara, A. Kimura, K. Miyamoto, T. Okuda, H. Namatame, M. Taniguchi, R. Arita, N. Nagaosa, K. Kobayashi, Y. Murakami, R. Kumai, Y. Kaneko, Y. Onose, and Y. Tokura, Nat. Mater. **10**, 521 (2011).
[21] A. Manchon, H. C. Koo, J. Nitta, S. Frolov, and R. A. Duine, Nat. Mater. **14**, 871 (2015).
[22] Y. A. Bychkov and E. I. Rashba, JETP Lett. **39**, 78 (1984).
[23] T. Oguchi and T. Shishidou, J. Phys. Condens. Matter **21**, 092001 (2009).
[24] E. Frantzeskakis and M. Grioni, Phys. Rev. B **84**, 155453 (2011).
[25] M. Nagano, A. Kodama, T. Shishidou, and T. Oguchi, J. Phys. Condens. Matter **21**, 064239 (2009).
[26] K. Sakamoto, T.-H. Kim, T. Kuzumaki, B. Muller, Y. Yamamoto, M. Ohtaka, J. R. Osiecki, K. Miyamoto, Y. Takeichi, A. Harasawa, S. D. Stolwijk, A. B. Schmidt, J. Fujii, R. I. G. Uhrberg, M. Donath, H. W. Yeom, and T. Oda, Nat. Commun. **4**, 2073 (2013).
[27] P. Roushan, J. Seo, C. V. Parker, Y. Hor, D. Hsieh, A. Richardella, M. Hasan, R. Cava, and A. Yazdani, Nature (London) **460**, 1106 (2009).
[28] H. Sakama and A. Kawazu, Surf. Sci. **342**, 199 (1995).
[29] H. Oyama and T. Ichikawa, Surf. Sci. **357–358**, 476 (1996).
[30] A. E. Dolbak, R. A. Zhachuk, and B. Z. Olshanetsky, Central Eur. J. Phys. **2**, 254 (2004).
[31] Y. K. Kim, J. R. Ahn, E. S. Cho, K.-S. An, H. W. Yeom, H. Koh, E. Rotenberg, and C. Park, Surf. Sci. **596**, L325 (2005).
[32] T. Okuda, Y. Takeichi, Y. Maeda, A. Harasawa, I. Matsuda, T. Kinoshita, and A. Kakizaki, Rev. Sci. Instrum. **79**, 123117 (2008).
[33] J. P. Perdew, J. A. Chevary, S. H. Vosko, K. A. Jackson, M. R. Pederson, D. J. Singh, and C. Fiolhais, Phys. Rev. B **46**, 6671 (1992).
[34] P. Hohenberg and W. Kohn, Phys. Rev. **136**, B864 (1964).
[35] K. Laasonen, A. Pasquarello, R. Car, C. Lee, and D. Vanderbilt, Phys. Rev. B **47**, 10142 (1993).
[36] M. A. V. Hove, W. Moritz, H. Over, P. J. Rous, A. Wan-der, N. M. A. Barvieri, U. Starke, and G. Somorjai, Surf. Sci. Rep. **19**, 191 (1993).
[37] See Supplemental Material at http://link.aps.org/supplemental/10.1103/PhysRevLett.117.016803 for details.
[38] J. B. Pendry, J. Phys. C **13**, 937 (1980).
[39] K. Sakamoto, M. Setvin, K. Mawatari, P. E. J. Eriksson, K. Miki, and R. I. G. Uhrberg, Phys. Rev. B **79**, 045304 (2009).
[40] I. Ivanov, A. Mazur, and J. Pollmann, Surf. Sci. **92**, 365 (1980).
[41] P. Höpfner, J. Schäfer, A. Fleszar, J. H. Dil, B. Slomski, F. Meier, C. Loho, C. Blumenstein, L. Patthey, W. Hanke, and R. Claessen, Phys. Rev. Lett. **108**, 186801 (2012).